Catalytic Isolation and Physicochemical Properties of Nanocrystalline Cellulose (NCC) using HCl-$FeCl_3$ System Combined with Ultrasonication

Sharifah Bee Abd Hamid, Zaira Z. Chowdhury,* Md. Ziaul Karim, and Md. Eaqub Ali

This research emphasizes the isolation of nanocrystalline cellulose (NCC) from palm tree cellulose (PTC) and α-cellulose (AC), using acidic $FeCl_3$-assisted catalytic pretreatment coupled with ultrasonication. The cavitation effect of ultrasonication affects the microstructure of the fibers, ultimately enhancing the crystallinity index of the prepared nanocrystalline cellulose (NCC) sample. In this research, Fourier transform infrared spectroscopy (FTIR) was used to identify the specific functional groups on both types of NCC sample. X-ray diffraction (XRD) analysis demonstrated that the isolated NCC from PTC and AC showed a higher crystallinity index of 73.51% and 89.03%, with diameters of 20 to 70 nm and 15 to 50 nm, respectively. The change in surface morphological features was observed by scanning electron microscopy (SEM), atomic force microscopy (AFM), and transmission electron microscopic (TEM) analysis. It was observed that PTC-based NCC had higher thermal stability than the starting cellulosic sample, whereas NCC isolated from AC showed an opposite trend of reduced thermal stability relative to the raw sample. The results indicated that catalytic acid hydrolysis with ultrasonication was able to yield up to 80.88% and 81.20% of NCC from PTC and AC, respectively, which is comparatively high enough for economic viability of the process.

Keywords: Hydrolysis; Palm Tree Cellulose (PTC); α-Cellulose (AC); Nanocrystalline cellulose (NCC); Ultrasonication

*Contact information: Nanotechnology and Catalysis Research Center (NANOCAT), University Malaya, Kuala Lumpur 50603, Malaysia; *Corresponding author: zaira.chowdhury76@gmail.com; dr.zaira.chowdhury@um.edu.my*

INTRODUCTION

Cellulose, the linear chain polysaccharide, is one of the most abundantly available natural resources. Presently it has become a promising substitute for sustainable extraction of value added chemicals and fuels (Wang *et al.* 2006). Plant cell walls are made of around 40 to 50% cellulose, which is surrounded by hemicellulose and embedded inside a lignin matrix (Hult *et al.* 2000). The polymer chain of cellulose consists of β-D-glucopyranose units linked by β-1,4 glycosidic linkages (Chowdhury *et al.* 2014). The chemical formula of cellulose is $(C_6H_{10}O_6)_n$, and it consists of a straight chain containing from several hundred to over ten thousand D-anhydro glucopyranose units (Chirayil *et al.* 2014). Physicochemical properties and crystalline packing of cellulose is regulated by intra- and intermolecular hydrogen bonding between the hydroxyl groups of these units (Fig. 1). The dimension of cellulose is mainly dependent on its origin as well as the preparation methods and conditions implemented during the extraction process (Liu *et al.* 2014). The molecular chain of cellulose contains crystalline and amorphous regions. The accessibility of a

chemical reagent inside the amorphous region is easier than in the crystalline region due to the more compact structure of the crystals (Jeoh *et al*. 2007).

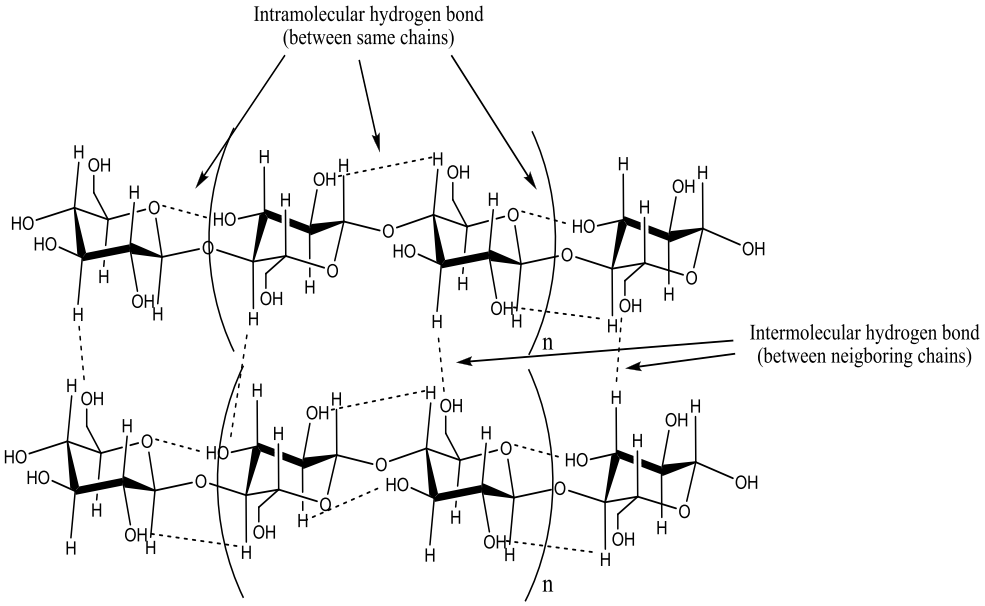

Fig. 1. Chemical structure of cellulose chains with intra- and intermolecular hydrogen bonds

Nano-dimensional cellulose is often referred to as cellulose nanocrystals, nano-whiskers, micro-fibrillated cellulose, microfibril aggregates, or nanofibers (Samir *et al.* 2005; Eichhorn *et al.* 2010; Siró and Plackett 2010). These are characterized with some unique properties such as a large surface area, excellent mechanical properties including high tensile strength and high Young's modulus, low coefficient of thermal expansion, high aspect ratio, non-toxic nature, and biodegradability (Nishino *et al.* 2004; Samir *et al.* 2005; Helbert *et al.* 1996). They are incorporated as reinforcing agents in polymer nanocomposites, which have potential applications in tissue engineering (Klemm *et al.* 2005; Moon *et al.* 2011; Saito *et al.* 2011; Jiang *et al.* 2013; Pirani and Hashaikeh 2013; Abdul Khalil *et al.* 2014). Due to optical transparency, as well as high mechanical and gas barrier properties, NCC is used to fabricate transparent films (Yousefi *et al.* 2011; Huang and Fu 2013). It is widely used in medicine, catalysis, textiles, surface coatings, drug delivery, and food packaging (Klemm *et al*. 2005; Deng *et al*. 2010; Das *et al.* 2011; Sacui *et al.* 2014). Until recently, cellulose nanoparticles have been extracted using different methods including mechanical treatments, such as steam explosion (Deepa *et al.* 2011), cryo-crushing (Chakraborty *et al.* 2005), ultrasonication (Li *et al.* 2012a), and high pressure homogenizing (Li *et al.* 2012b), as well as chemical treatments using acid or alkali (Bendahou *et al.* 2010; Johar *et al.* 2012; Zaman *et al.* 2012), biological treatments such as enzyme-assisted hydrolysis (Henriksson *et al.* 2007), micro-fluidization (Ferrer *et al.* 2012), and TEMPO-mediated oxidation (Benhamou *et al.* 2014). However, to obtain specific properties, a combination of two or several of those methods can be incorporated. Concentrated sulfuric acid is frequently used to isolate NCC from different lignocellulosic sources. However, this process suffers from several drawbacks such as a low yield of NCC, which is usually lower than 50% (Li *et al.* 2014a). This results in potential degradation of cellulose and generation of a huge amount of liquid slurry as wastage. This makes

the process not ecofriendly enough, as processing the slurry containing concentrated acid is difficult. Although much attention has been given for extraction of NCC by numerous methods, the combination of ultrasonic treatment and application of transition metal ion catalyst for acid hydrolysis using moderately concentrated acid has been rarely stated.

Recently, ultrasonication was used as an emerging method to obtain nanocrystalline cellulose without the significant impact on fiber properties (Tang *et al.* 2013; Chen *et al.* 2013). During ultrasonication, a strong mechanical oscillating energy is produced by high-intensity ultrasonic waves (Chen *et al.* 2011). The energy provided by cavitation is approximately, 10 to 100 kJ/mol - that can effectively break down the interaction forces between cellulose microfibers, facilitating the disintegration of cellulosic fibers into nanofibers (Tischer *et al.* 2010). We have earlier found that addition of a metal ion for pretreatment of cellulose was effective for selective hydrolysis of the amorphous region of cellulose to ensure a high yield of MCC (Hamid *et al.* 2014). Hence, the combination of ultrasound and metal ion-based acid hydrolysis method was applied to isolate NCC in this study.

The above perusal of the literature reflects that, until now, no studies have been conducted for the preparation of nanocrystalline cellulose (NCC) maintaining high yield and crystallinity index using ultrasonication-assisted transition metal ion catalyzed acid hydrolysis process from palm tree cellulose (PTC) and α-cellulose. In this study, NCC was successfully isolated by the $FeCl_3$-catalyzed acid hydrolysis process combined with the ultrasonication treatment. The characteristic of NCC structure was determined by Fourier transform infrared (FTIR) spectroscopy. The morphological features and crystallinity of the obtained NCC samples were characterized by scanning electron microscopy (SEM), transmission electron microscopy (TEM), atomic force microscopy (AFM), and X-ray diffraction (XRD) techniques. Thermogravimetric analysis (TGA) was used to determine the thermal stability of the extracted NCC sample.

EXPERIMENTAL

Materials

The palm tree cellulose (PTC) was supplied commercially by the Malaysian Palm Oil Board (MPOB); the cellulose was extracted from palm tree trunk (PTT). Commercial α-cellulose (AC) was supplied by Sigma Aldrich. Iron (III) chloride hexahydrate and fuming (37%) hydrochloric acid were purchased from R & M Chemicals and Merck, Germany respectively.

Methods

Pretreatment of cellulose

0.8 mol/L iron (III) chloride solution was prepared in 3 mol/L HCl acid. The solution was taken in a 50 mL round bottom flask. 1.0 g of PTC sample was added into the round bottom flask and stirred over a magnetic hot plate at 98 °C for 4 h (Karim *et al.* 2014). Preliminary screening studies showed that, under the same preparation condition, the yield for α-cellulose (AC) dropped significantly. That is why the process parameters were optimized to ensure higher yield percentage as well as crystallinity index for α-cellulose. In the case of AC, 1.28 mol/L $FeCl_3$ solution was prepared in 2.5

mol/L hydrochloric acid; 1.0 g of AC was taken with the prepared solution and stirred over a hot plate at 80 °C for 3.8 h (Hamid *et al.* 2014).

Isolation of nanocrystalline cellulose (NCC)

The resulting suspensions from both the sample were treated using a UIP1000hd transducer ultrasonicator with a constant amplitude of 80% for 20 min in an ice-water bath. The milky colloidal suspension was centrifuged, and centrifugation process was repeated until the pH of the suspension was neutral. A certain amount (mL) of the samples was dried at 105 °C to a constant weight. The yield (%) was calculated according to Eq. 1,

$$\text{Yield (\%)} = \frac{M_1 \times M_3}{M_2 \times M_0} \times 100 \quad (1)$$

where M_0 is the mass of sample taken, M_1 is the weight of the dry powder finally obtained, M_2 is the mass of the suspension sample used to get the dry powder, and M_3 is the mass of the suspension in the final preparation (Karim *et al.* 2014). The suspension was dried with a freeze dryer. The dried sample was stored for subsequent characterization. The obtained products were denoted as UH-PTC and UH-AC for palm tree cellulose and α-cellulose, respectively. The samples prepared without ultrasonication were denoted as H-PTC and H-AC.

Physicochemical characterization of NCC

Fourier transform infrared spectroscopy was used to identify functional groups of fibers using a Bruker IFS 66/S (Bruker, Germany) spectrophotometer. A small amount of powder sample was blended with KBr at a fixed ratio to fabricate a translucent disc. The spectra for each sample was taken in the range of 400 to 4000 cm^{-1}.

X-ray diffraction patterns of the samples were examined by Bruker AXSD8 ADVANCE (Bruker, Germany) X-ray diffractometer using Cu Kα radiation (λ = 0.1540 nm). The scattered radiation was detected in the angle range 5 to 45°. The crystallinity index was calculated according to Eq. 2 (Bendahou *et al.* 2009; Terinte *et al.* 2011):

$$\text{CrI} = \frac{(I_{002} - I_{am})}{I_{002}} \times 100 \quad (2)$$

Here, *CrI* is the crystallinity index, I_{002} is the maximum intensity of the 200 peak at 2θ = 22.5°, and I_{am} is the intensity at 2θ = 18.7°.

The crystalline dimension (nm) of each sample was calculated by using Scherrer Eq. 3 (Yahya *et al.* 2014),

$$D = \frac{0.9\lambda}{\beta_{hkl} \cos\theta_{hkl}} \quad (3)$$

where θ is the diffraction angle, λ = 0.154 nm, and β_{hkl} is the corrected angular width in radians at half maximum intensity of the 200 peak.

Surface morphology of the fibers was observed by using a FEI Quanta 200F (FEI Company, USA) scanning electron microscope operated at 10 kV. The sample surfaces were coated with gold before observation.

A drop of dilute suspension (0.01% w/v) of nanocrystalline cellulose was deposited onto freshly cleaved mica and dried in a vaccum oven at 60 °C prior to atomic force microscopy (BioScope Catalyst, Bruker Nano Surfaces Division, USA) examination. Images were collected using tapping mode at the room temperature with a silicon cantilever.

Transmission electron microscopy (Hitachi HT7700, Tokyo, Japan) was carried out using an accelerating voltage of 80 kV to determine the dimensions of cellulose nanocrystals. A drop of a diluted nanocrystalline cellulose suspensions (0.005% w/v) was deposited over a carbon-coated copper grid and allowed to dry at ambient temperature before TEM analysis. ImageJ 1.49r software (Wayne Rasband, National Institutes of Health, USA) was used to determine the width of nanocrystalline cellulose from the TEM images. Around forty partials were randomly selected, and the histograms of NCC width were designated by OriginPro 9.0.0 software (SR2 b87, OriginLab Corp., Northampton, USA).

Thermogravimetric analysis (TGA) was carried out using a PerkinElmer, (TGA 4000, USA) instrument in order to characterize the thermal stability of the cellulose samples. Approximately 5.0 mg of each sample was heated from room temperature to 550 °C under nitrogen atmosphere at a heating rate of 10 °C/min. All measurements were performed using nitrogen gas flow of 50 mL/min.

RESULTS AND DISCUSSION

The chemical groups of untreated, hydrolyzed, and ultrasonicated PTC and AC cellulose were identified using FT-IR spectra (Fig. 1). The FTIR spectra of ultrasonically treated cellulose were similar to those of the untreated and hydrolyzed cellulose samples. The absorption band around 3400 cm^{-1} was related to the inter-molecular and intra-molecular O-H stretching vibration band.

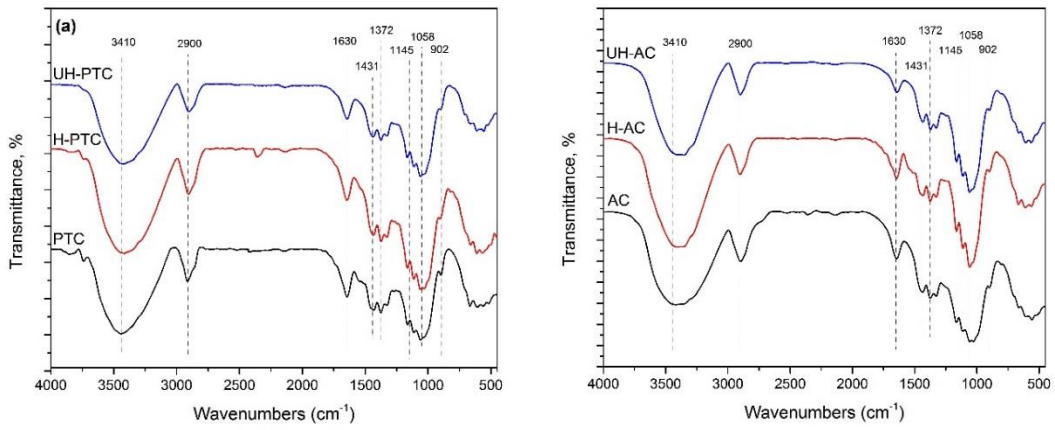

Fig. 2. FTIR spectrum under different stages of (a) PTC and (b) AC

The peaks detected at 2900 cm^{-1} are associated with CH_2 groups of cellulose (Haafiz *et al.* 2014). A peak around 1600 cm^{-1} is principally attributed to H-O-H stretching vibration of absorbed water molecules in carbohydrate (Karim *et al.* 2014). The results were in agreement with previous findings, from a study in which nanocrystalline cellulose was extracted using $NiNO_3 \cdot 6H_2O$ and H_2SO_4 acid from microcrystalline cellulose and dried jute stalk (Yahya *et al.* 2014; Chowdhury and Abd

Hamid 2015). A small peak detected at 1428 to 1433 cm^{-1} is associated with intermolecular hydrogen bonding at the C_6 group (Kumar *et al.* 2002). Moreover, the peak appearing around the 1300 cm^{-1} range in the spectra of all samples is attributed to C-H bending and C-O symmetric stretching within the polysaccharide aromatic rings (Haafiz *et al.* 2014). The absorption bands at 1058 and 902 cm^{-1} are due to C-O-C stretching vibrations, which are considered as the typical bonds of cellulose (Sun *et al.* 2000). The peak near 1145 cm^{-1} signifies glycosidic linkages of cellulose chain. The minor peaks appearing around 1410-1423, 1310-1335, 1223-1241, 1105-1108, 1010-1024, and 899-910 cm^{-1} are related to the characteristic cellulosic bands inside the sample (Sun *et al.* 2005). Overall, there was a slight change in the intensity of some peaks after consecutive acid hydrolysis and ultrasonic treatment. No obvious difference could be found in the FTIR spectra. The above observation showed that the acid hydrolysis with or without ultrasonication did not disrupt the chemical structure of cellulose molecule. This phenomenon was further confirmed with XRD analysis.

XRD studies for untreated PTC and AC along with cellulosic samples after hydrolysis (H-PTC and H-AC) and ultrasonication treatment (UH-PTC and UH-AC) were conducted to investigate the crystalline behavior of these samples, and results are shown in Fig. 3. All the diffractograms for both the samples showed two distinctive peaks around 2θ = 14.0° to 16.0° and 22.0° to 24.0°, which represents typical cellulose I structure (Nishiyama *et al.* 2003). The peak around 22.0° to 24.0° is the primary peak of cellulose, which represents the crystalline region of cellulose, whereas the peak around 2θ = 14.0° to 16.0° is denoted as secondary peak for amorphous region of cellulose (Liu *et al.* 2012). Thus, it can be concluded that the crystal structure of cellulose was not disrupted after combined treatment using catalytic acidic iron chloride and ultrasonication (Li *et al.* 2011).

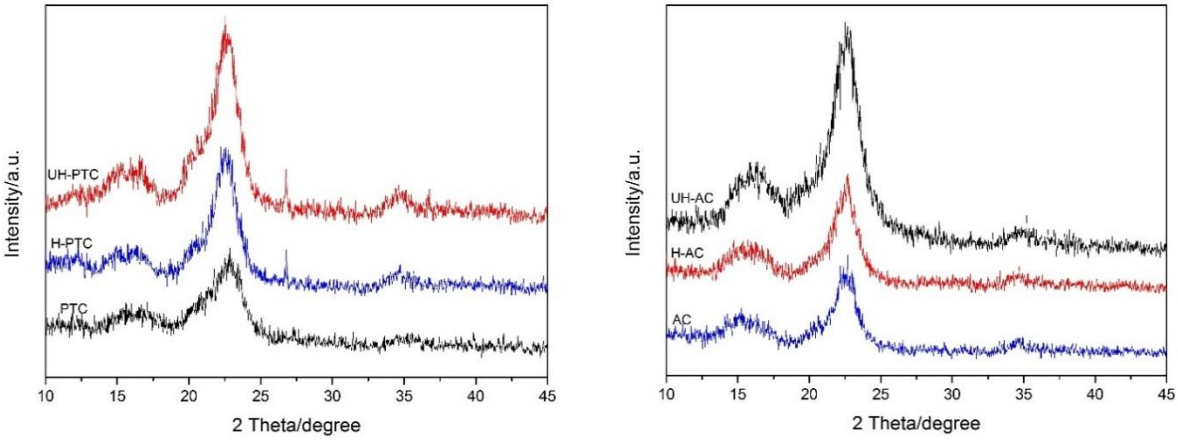

Fig. 3. X-ray Diffraction patterns under different treatments of (a) PTC and (b) AC

After catalytic acidic iron chloride treatment, the crystallinity index for both the samples (H-PTC and H-AC) increased to a certain extent. The increase in crystallinity index might be attributed to the partial dissolution of the amorphous region of the cellulosic samples. Moreover, the isolated nanocrystalline cellulose after ultrasonication process (UH-PTC and UH-AC) for 20 min in the presence of water showed a yet higher crystallinity index (Table 1). The untreated PTC has a crystallinity index of 52.36%, which after hydrolysis and ultrasonication became 68.66% and 73.51%, respectively. However, ultrasonication using AC provided an NCC sample with higher crystallinity index (89.03%) than the PTC sample. The similarity of diffractograms obtained from both the samples, hydrolyzed and with and without sonication, indicated that successive

treatment could not alter the main crystallite structure of cellulose. These results revealed that ultrasonication can increase the crystallinity of cellulose. The cavitation effect of ultrasonication can damage the amorphous regions as well as create localized erosion on the surface, leading to acceleration of the chain fragmentation process (Caruso *et al.* 2009).

Ultrasonic cavitation ensures morphological changes in cellulose by enhancing its hygroscopicity, which subsequently facilitates diffusion of the solvent easily (Cintas and Luche 1999; Tang *et al.* 2005; Li and Renneckar 2009; Moon *et al*. 2011; Chowdhury and Abd Hamid 2015). The intense collapse of micro-bubbles gives rise to microjets over the surface of the cellulose. This would cause erosion, resulting in defibrillation of the cellulose molecule by breaking the hydrogen bond inside the fiber matrix. Overall, the process would initiate gradual disintegration of the micro-dimensional cellulose fibers into nanofibers (Tischer *et al.* 2010).

Table 1. Crystallinity Index of PTC, AC, and their Respective Samples

Samples	Crystallinity index (%)	Average Crystalline Dimension (nm)
PTC	52.36	10.4
H-PTC	68.66	28.1
UH-PTC	73.51	34.8
AC	68.37	20.5
H-AC	86.98	30.9
UH-AC	89.03	52.2

Table 1 summarizes the average crystalline dimension with crystallinity index of all the samples. The increase in the crystalline dimension of cellulose after successive treatments predominantly revealed the narrowing of the crystallite size distribution. The crystallite sizes increased after successive treatment of acid hydrolysis and ultrasonication.

A similar phenomenon was reported during extraction of NCC from waste newspaper (Mohamed *et al.* 2015). Crystallinity percentage plays a vital role to enhance the tensile strength and stiffness of the cellulosic fiber due to the compact molecular structure of cellulose. This reflects the presence of a highly ordered crystalline domain of cellulose, which can further enhance Young's modulus along the longitudinal directions (Li *et al.* 2014b; Chowdhury *et al.* 2015). Thus, it can be concluded that the combined application of acid hydrolysis with ultrasonication would be effective to obtain nanocrystalline cellulose (NCC). Thus it can be used as a better reinforcing agent in nano-composite preparation.

Thermogravimetric (TG) and derivatives of thermogravimetric (DTG) curves of PTC and AC with their corresponding nanocrystalline cellulose, UH-PTC, and UH-AC, is shown in Fig. 4. Below 110 °C, all samples lost a small amount of weight due to the evaporation of absorbed water.

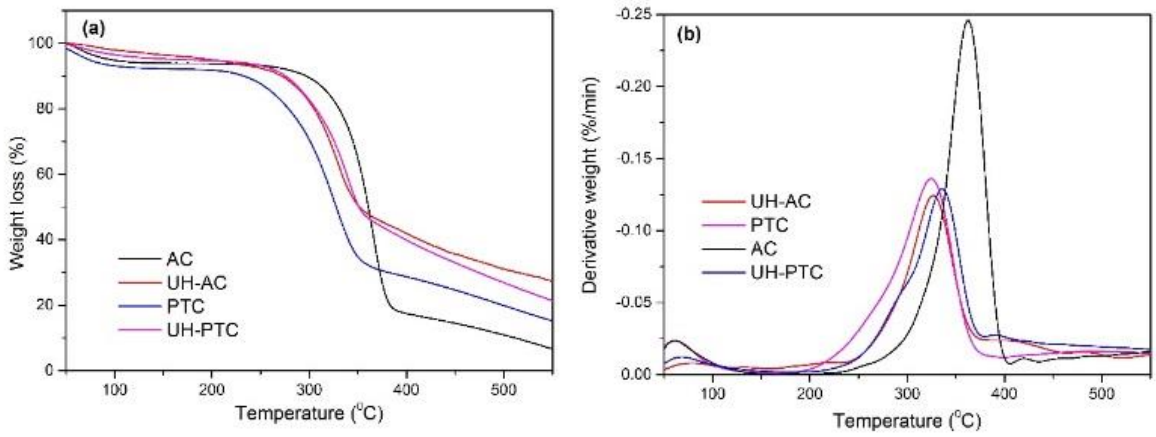

Fig. 4. Thermogravimetric (TG) curves (a) and of Differential Thermogravimetric (DTG) curves (b) for PTC, AC, UH-PTC, and UH-AC

The PTC showed a typical decomposition behavior with an onset degradation temperature (T_0) of 195.0 °C, and the maximum thermal degradation temperature (T_{max}) occurring at 320.0 °C. The degradation of the PTC had only one pyrolysis process in the DTG curve. The main mass loss step for PTC was observed in the range of 195.0 to 355.0 °C. The char yield around 550.0 °C was 15.2%. On the other hand, the onset temperature (T_0) and maximum thermal degradation temperature (T_{max}) for UH-PTC was observed at a relatively higher temperature of 228.0 °C and 336.0 °C, respectively (Fig. 4a). The rearrangement and reorientation of the crystals, as well as dissolution of amorphous region of cellulosic chain, offers to increase the onset and maximum thermal degradation temperature (Mandal and Chakrabarty 2011). The results obtained here regarding higher thermal stability of the extracted nanocrystalline cellulose were in agreement with the previous work carried out using jute and pineapple leaf fiber (Abraham *et al.* 2011). The char residue obtained for UH-PTC was relatively higher, nearly 21.4%, at 550.0 °C. This demonstrated that UH-PTC has better thermal stability compared to PTC. Higher decomposition temperature for UH-PTC illustrated greater crystallinity of the prepared nanocrystalline cellulose sample (Rosa *et al.* 2012). This observation was further supported by XRD analysis, where the crystallinity of UH-PTC determined was higher than the PTC sample.

For the AC (Fig. 4a) sample, the onset degradation temperature (T_0) was observed at 228.0 °C. There was 6.6% char yield at 550 °C. The maximum thermal degradation temperature (T_{max}) occurred at 360.0 °C. The degradation of the AC occurred within a relatively narrow temperature range and had only one pyrolysis process in the DTG curve. The main mass loss step for AC was observed within the range of 228.0 to 398.0 °C. The onset degradation temperature (T_0) for UH-AC was observed at relatively lower temperature of 196.0 °C. The degradation of UH-AC occurred within a broader temperature range of 196.0 to 350.0 °C compared to AC. Similarly for UH-AC, the char residue obtained was around 27.5% at 550 °C, which was higher than the char yield of AC. The maximum thermal degradation temperature (T_{max}) of UH-AC was 327 °C (Fig. 4b). The thermal decomposition of UH-AC shifted to lower temperatures and happened within broader temperature ranges, reflecting lower thermal stability of the nanocrystalline cellulose sample extracted from AC. This was obvious due to the nano-size and larger number of free ends of cellulosic chains inside the sample (Li *et al*. 2011).

The surface morphology of PTC and AC, with their corresponding hydrolyzed and ultrasonicated samples, is shown by scanning electron microscopic (SEM) images. Figures 5-a and 5-b show the starting cellulosic sample before treatment.

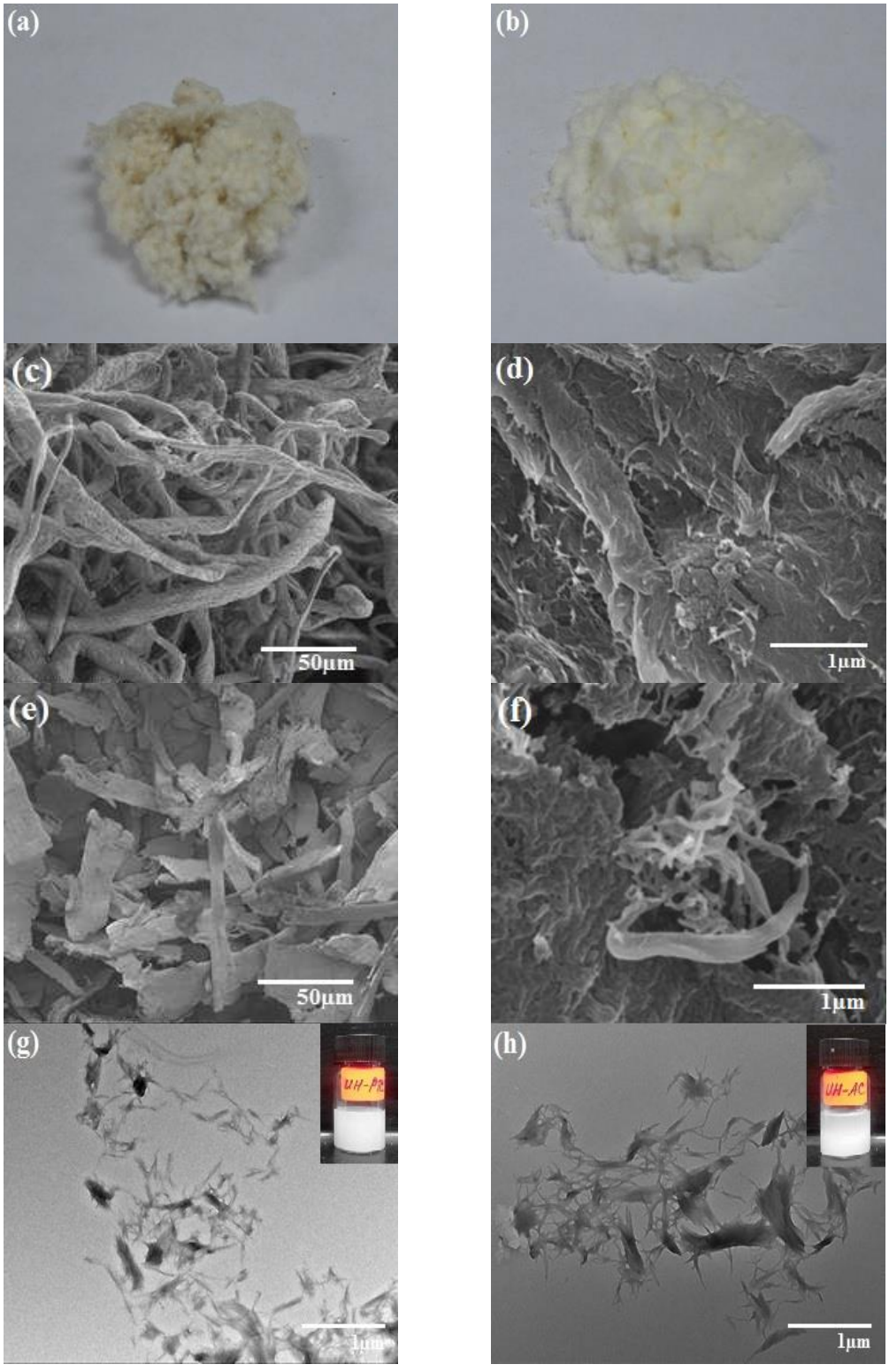

Fig. 5. (a) Untreated PTC, (b) Untreated AC, (c) SEM images of Untreated PTC, (d) SEM images of UH-PTC, (e) SEM images of Untreated PTC, (f) SEM images of UH-AC, (g) TEM images of UH-PTC, and (h) TEM images of UH-AC

The raw samples of PTC and AC before treatments were long, fibrillated, and had irregular shapes (Fig. 5-c and 5-e). The surface of PTC was comparatively rough and uneven with folding, compared to the AC sample. After subsequent acidic ferric chloride hydrolysis and ultrasonic treatments, the fibers were broken down to a great extent and produced their respective UH-PTC and UH-AC (Fig. 5-d and 5-f). It is apparent that UH-PTC and UH-AC displayed a uniform rod-like shape, which was further supported by TEM images (Fig. 5-g and 5-h). The width of UH-PTC and UH-AC were about 20 to 70 nm and 15 to 50 nm, respectively (Figs. 6-a and 6-b). The shape and dimensions of the cellulose nanocrystals were found to be fairly similar. During ultrasonic cavitation, solvodynamic shear force is produced, which causes the nucleation, growth, and collapse of microbubbles inside the solution (Caruso *et al.* 2009). This works over the surface of the fibers, eroding and cracking the surface; finally it will result in the scission of cellulose polymer bonds to produce nanocellulose.

From TEM images, it was observed that the nanocrystalline cellulose particles were aggregated to some extent, which can be attributed to the evaporation of water. The lateral aggregation of cellulose nanocrystals in TEM images is expected. A similar phenomenon was observed for extraction of nanocrystalline cellulose from soy hulls (Neto *et al.* 2013). The aggregation might take place due to high surface area or strong hydrogen bonding between the nano-whiskers of cellulose (Neto *et al.* 2013). Even these aggregates can exist in suspension, but when the dispersing medium is evaporated during sample preparation for TEM, bundles of whiskers can be more apparent than individual needles of nanocrystalline cellulose (Elazzouzi-Hafraoui *et al.* 2008).

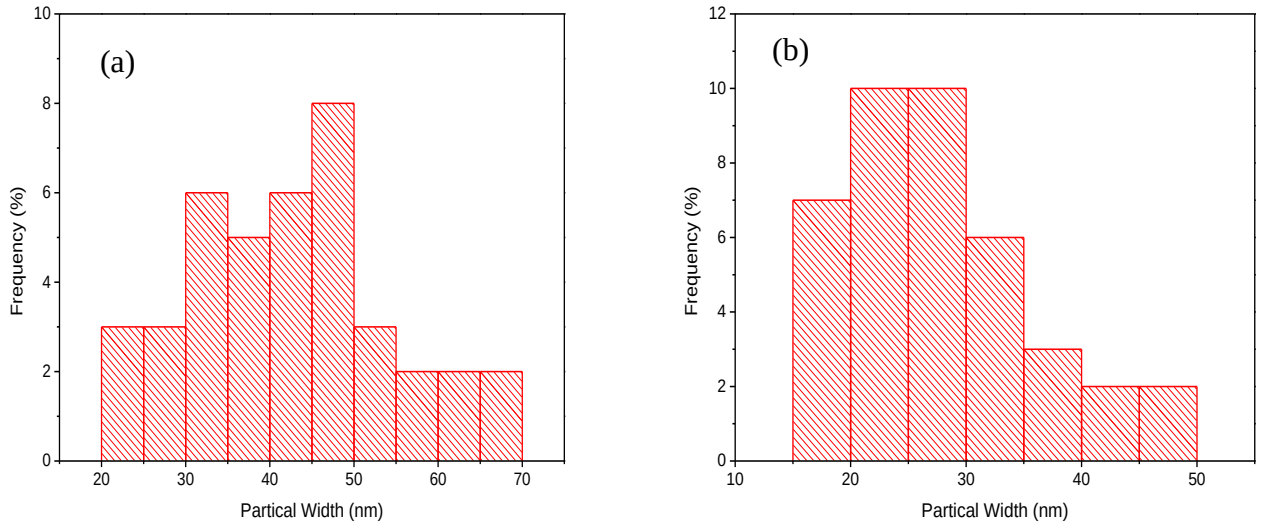

Fig. 6. NCC size distribution profile (frequency *vs*. fiber diameter (nm) (a) UH-PTC (b) UH-AC

AFM images of nanocrystalline cellulose extracted from PTC and AC samples are shown in Fig. 7. Nano-dimensional rod-shape or needle-like nanoparticles were observed from AFM 3D and height profiles. The images show that the UH-PTC was more agglomerated than UH-AC. These results correlate well with the TEM measurements. This indicated that catalytic acid hydrolysis together with ultrasonication was able to cleave long cellulose microfibers into nanocrystalline cellulose, ultimately resulting in the reduction of dimensions from micron to nanometer.

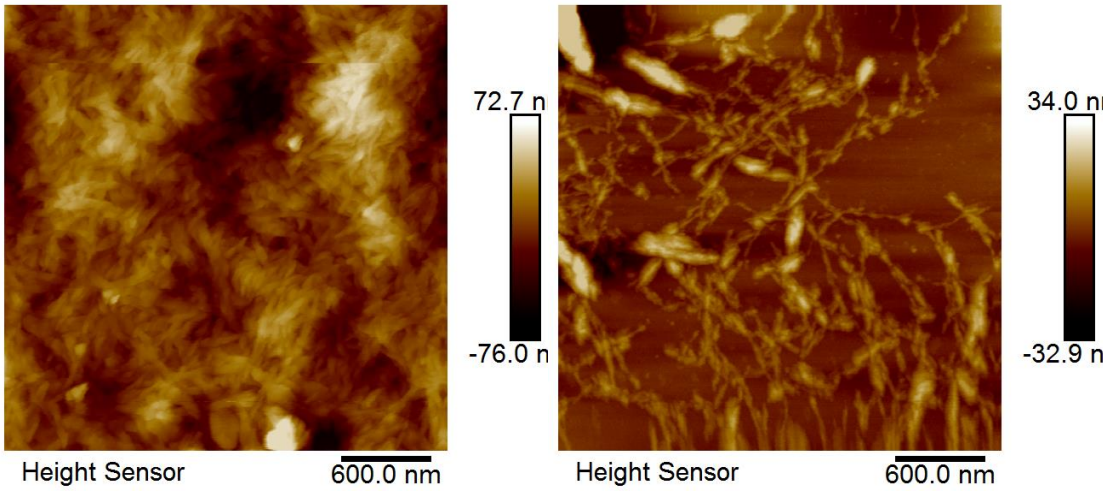

Fig. 7. AFM images of (a) UH-PTC and (b) UH-AC

CONCLUSIONS

1. Catalytic acid hydrolysis was combined with simple ultrasonication treatment to obtain nanocrystalline cellulose (NCC) from palm tree cellulose and α-cellulose.
2. The yield obtained for both the PTC and AC samples was high, around 80.88% and 81.20%, respectively, which contributes to making the process economically feasible.
3. AC showed a higher crystallinity index of 89.03% than PTC, which exhibited a crystallinity index of 73.51%.
4. The nano-rod like structure of NCC was confirmed by TEM and AFM analysis. Nanocrystalline cellulose (NCC) isolated after ultrasonication of PTC and AC, and had diameters of 20 to 70 nm and 15 to 50 nm respectively.
5. The basic surface functional groups of cellulosic structures were retained after successive treatments, reflecting that no chemical transformation had occurred during the extraction, only selective hydrolysis of amorphous region and defragmentation, resulting in NCC samples with higher crystallinity index.

ACKNOWLEDGEMENTS

The authors would also like to thank High Impact Research (HIR F-000032) of University Malaya, Malaysia for their cordial support to complete this work.

REFERENCES CITED

Abdul Khalil, H. P. S., Davoudpour, Y., Islam, M. N., Mustapha, A., Sudesh, K., Dungani, R., and Jawaid, M. (2014). "Production and modification of nanofibrillated cellulose using various mechanical processes: A review," *Carbohydr. Polym.* 99, 649-665. DOI: 10.1016/j.carbpol.2013.08.069

Azizi Samir, M. A. S., Alloin, F., and Dufresne, A. (2005). "Review of recent research into cellulosic whiskers, their properties and their application in nanocomposite field," *Biomacromolecules* 6(2), 612-626. DOI:612-626. 10.1021/bm0493685.

Abraham, E., Deepa, B., Pothan, L. A., Jacob, M., Thomas, S., Cvelbar, U., and Anand, R. (2011). "Extraction of nanocellulose fibrils from lignocellulosic fibres: A novel approach," *Carbohydr. Polym.* 86(4) 1468-1475. DOI.10.1016/j.carbpol.2011.06.034.

Bendahou, A., Habibi, Y., Dufresne, A., and Kaddami, H. J. (2009). "Biobased MatPhysico-chemical characterization of palm from *Phoenix dactylfera* - L, preparation ofcellulose whiskers and natural rubber-based nanocomposites," *J. Biobased Mat.* 3(1), 81-90, DOI: 10.1166/jbmb.2009.2011.

Bendahou, A., Kaddami, H., and Dufresne, A. (2010). "Investigation on the effect of cellulosic nanoparticles' morphology on the properties of natural rubber based nanocomposites," *European Polymer Journal* 46(4), 609-620. DOI: 10.1016/j.eurpolymj.2009.12.025.

Benhamou, K., Magnin, A., Mortht, G., Dufresne, A., and Kaddami. H. (2014). "Size and viscoelastic properties control of NFC from palm tree by monitoring TEMPO-mediated oxidation time," *Carbohydr. Polym.* 99(2), 74-83. DOI: 10.1016/j.carbpol.2013.08.032.

Caruso, M. M., Davis, D. A., Shen, Q., Odom, S. A., Sottos, N. R., White, S. R., and Moore, J. S. (2009). "Mechanically-induced chemical changes in polymeric materials," *Chem. Rev.* 109(11), 5755-5798. DOI:10.1021/cr9001353.

Cintas, P., and Luche, J. L. (1999). "Green chemistry: The sonochemical approach," *Green Chem.* 1(3), 115-125. DOI: 10.1039/A900593E.

Chakraborty, A., Sain, M., and Kortschot, M. (2005). "Cellulose microfibrils: A novel method of preparation using high shear refining and cryocrushing," *Holzforschung* 59(1), 102-107. DOI:10.1515/Hf.2005.016

Chen, P., Yu, H., Liu, Y., Chen, W., Wang, X., and Ouyang, M. (2013). "Concentration effects on the isolation and dynamic rheological behavior of cellulose nanofibers via ultrasonic processing," *Cellulose* 20(1), 149-157. DOI:10.1007/s10570-012-9829-7

Chen, W., Yu, H., Liu, Y., Chen, P., Zhang, M., and Hai, Y. (2011). "Individualization of cellulose nanofibers from wood using high-intensity ultrasonication combined with chemical pretreatments," *Carbohydr. Polym.* 83(4), 1804-1811. DOI:10.1016/j.carbpol.2010.10.040

Chirayil, C. J., Joy, J., Mathew, L., Mozetic, M., Koetz, J., and Thomas, S. (2014). "Isolation and characterization of cellulose nanofibrils from *Helicteres isora* plant," *Ind. Crops Prod.* 59, 27-34. DOI:10.1016/j.indcrop.2014.04.020

Chowdhury, Z. Z., Zain, S. M., Hamid, S. B. A., and Khalid, K. (2014). "Catalytic role of ionic liquids for dissolution and degradation of biomacromolecules," *BioResources* 9(1), 1787-1823. DOI:10.15376/biores.9.1.1787-1823.

Chowdhury, Z. Z., and Abd Hamid, S. B. (2015). "Preparation and characterization of nanocrystalline cellulose using ultrasonication combined with a microwave-assisted pretreatment process," *BioResources* (Accepted).

Das, K., Ray, D., Bandyopadhyay, N. R., Sahoo, S., Mohanty, A. K., and Misra, M. (2011). "Physicomechanical properties of the jute micro/nanofibril reinforced starch/polyvinyl alcohol bio-composite films," *Compos Part B* 42, 376-381. DOI:10.1016/j.compositesb.2010.12.017

Deng, H., Zhou, X., Wang, X., Zhang, C., Ding, B., Zhang, Q., and Du, Y. (2010). Layer-by- layer structured polysaccharides film coated cellulose nanofibrous mats for cell culture," C*arbohydr Polym* 80(2), 475-480. DOI:10.1016/j.carbpol.2009.12.004.

Deepa, B., Abraham, E., Cherian, B. M., Bismarck, A., Blaker, J. J., Pothan, L. A., Leao, S. F., de Souza, and Kottaisamy, M. (2011). "Structure, morphology and thermal characteristics of banana nano fibers obtained by steam explosion," *Bioresour. Technol.* 102(2), 1988-1997. DOI:10.1016/j.biortech.2010.09.030

Eichhorn, S. J., Dufresne, A., Aranguren,M., Marcovich, N. E., Capadona, J. R., Rowan, S. J., Weder, C., Thielemans, W., Roman, M., Renneckar, S., Gindl, W., Veigel, S., Keckes, J., Yano, H., Abe, K., Nogi, M., Nakagaito, A.N., Mangalam, A., Simonsen, J., Benight, A. S., Bismarck, A., Berglund, L. A., and Peijs, T. (2010). "Review: Current international research into cellulose nanofibres and nanocomposites," *J. Mater. Sci.* 45(1), 1-33. DOI:10.1007/s10853-009-3874-0

Elazzouzi-Hafraoui, S., Nishiyama, Y., Putaux, J. L., Heux, L., Dubreuil, F., and Rochas, C. (2008). "The shape and size distribution of crystalline nanoparticles prepared by acid hydrolysis of native cellulose," *Biomacromolecules* 9(1), 57-65. DOI: 10.1021/bm700769p.

Ferrer, A., Filpponen, I., Rodríguez, A., Laine, J., and Rojas, O. J. (2012). "Valorization of residual Empty Palm Fruit Bunch Fibers (EPFBF) by microfluidization: Production of nanofibrillated cellulose and EPFBF nanopaper," *Bioresour. Technol.* 125, 249-255. DOI:10.1016/j.biortech.2012.08.108.

Haafiz, M. M., Hassan, A., Zakaria, Z., and Inuwa, I. (2014). "Isolation and characterization of cellulose nanowhiskers from oil palm biomass microcrystalline cellulose," *Carbohydr. Polym.* 103, 119-125. DOI:10.1016/j.carbpol.2013.11.055

Hamid, S. B. A., Chowdhury, Z. Z., and Karim, M. Z. (2014). "Catalytic extraction of Microcrystalline Cellulose (MCC) from *Elaeis guineensis* using Central Composite Design (CCD)," *BioResources* 9(4), 7403-7426. DOI:10.15376/biores.9.4.7403-7426.

Helbert, W., Cavaille, J., and Dufresne, A. (1996). "Thermoplastic nanocomposites filled with wheat straw cellulose whiskers. Part I: Processing and mechanical behavior," *Polymer Comp.* 17(4), 604-611. DOI:10.1002/pc.10650

Henriksson, M., Henriksson, G., Berglund, L., and Lindström, T. (2007). "An environmentally friendly method for enzyme-assisted preparation of microfibrillated cellulose (MFC) nanofibers," *Eur. Polym. J.* 43(8), 3434-3441. DOI:10.1016/j.eurpolymj.2007.05.038

Huang, Y.-B., and Fu, Y. (2013). "Hydrolysis of cellulose to glucose by solid acid catalysts," *Green Chem.* 15(5), 1095-1111. DOI:10.1039/c3gc40136g

Hult, E.-L., Larsson, P. T., and Iversen, T. (2000). "A comparative CP/MAS 13C-NMR study of cellulose structure in spruce wood and kraft pulp," *Cellulose* 7(1), 35-55. DOI: 10.1023/a:1009236932134

Johar, N., Ahmad, I., and Dufresne, A. (2012). "Extraction, preparation and characterization of cellulose fibres and nanocrystals from rice husk," *Ind. Crops Prod.* 37(1), 93-99. DOI:10.1016/j.indcrop.2011.12.016

Jeoh, T., Ishizawa, C. I., Davis, M. F., Himmel, M. E., Adney, W. S., and Johnson, D. K. (2007). "Cellulase digestibility of pretreated biomass is limited by cellulose accessibility," *Biotechnol. Bioeng.* 98(1), 112-122. DOI:10.1002/bit.21408

Jiang, F., Han, S., and Hsieh, Y. L. (2013). "Controlled defibrillation of rice straw cellulose and self-assembly of cellulose nanofibrils into highly crystalline fibrous materials," *RSC Adv.* 3(30), 12366-12375. DOI:10.1039/C3RA41646A

Karim, M. Z., Chowdhury, Z. Z., Hamid, S. B. A., and Ali, M. E. (2014). "Statistical optimization for acid hydrolysis of microcrystalline cellulose and its physiochemical characterization by using metal ion catalyst," *Materials* 7(10), 6982-6999. DOI:10.3390/ma7106982

Klemm, D., Heublein, B., Fink, H. -P., and Bohn, A. (2005). "Cellulose: Fascinating biopolymer and sustainable raw material," *Angewandte Chemie International Edition* 44(22), 3358-3393. DOI:10.1002/anie.200460587

Kumar, V., de la Luz Reus-Medina, M., and Yang, D. (2002). "Preparation, characterization, and tabletting properties of a new cellulose-based pharmaceutical aid," *Int. J. Pharm.* 235(1), 129-140. DOI:10.1016/S0378-5173(01)00995-4

Li, Q. Q., and Renneckar, S. (2009). "Molecularly thin nanoparticles from cellulose: Isolation of sub-microfibrillar structures," *Cellulose* 16(6), 1025-1032. DOI: 10.1007/s10570-009-9329-6.

Li, J., Wei, X., Wang, Q., Chen, J., Chang, G., Kong, L., Su, J., and Liu, Y. (2012b). "Homogeneous isolation of nanocellulose from sugarcane bagasse by high pressure homogenization," *Carbohydr. Polym.* 90(4), 1609-1613. DOI: 10.1016/j.carbpol.2012.07.038

Li, W., Wang, R., and Liu, S. (2011). "Nanocrystalline cellulose prepared from softwood kraft pulp via ultrasonic-assisted acid hydrolysis," *BioResources* 6(4), 4271-4281. DOI:10.15376/biores.6.4.4271-4281

Li, W., Yue, J., and Liu, S. (2012a). "Preparation of nanocrystalline cellulose via ultrasound and its reinforcement capability for poly (vinyl alcohol) composites," *Ultrason Sonochem* 19(3), 479-485. DOI:10.1016/j.ultsonch.2011.11.007

Li, Y., Zhu, H., Xu, M., Zhuang, Z., Xu, M., and Dai, H. (2014a). "High yield preparation method of thermally stable cellulose nanofibers," *BioResources* 9(2), 1986-1997. DOI:10.15376/biores.9.2.1986-1997.

Li, M., Wang, L., Li, D., Cheng, Y., and Adhikari, B. (2014b). "Preparation and characterization of cellulose nanofibers from de-pectinated sugar beet pulp," *Carbohydr. Polym.* 102(1), 136-143. DOI: 10.1016/j.carbpol.2013.11.021.

Liu, Y., Wang, H., Yu, G., Yu, Q., Li, B., and Mu, X. (2014). "A novel approach for the preparation of nanocrystalline cellulose by using phosphotungstic acid," *Carbohydr. Polym.* 110, 415-422. DOI:10.1016/j.carbpol.2014.04.040

Liu, J. G., Wang, Q. H., Wang, S., Dexun Zou, D. X., and Sonomoto, K. (2012). "Utilization of microwave-NaOH pretreatment technology to improve performance and L-lactic acid yield from vinasse," *Biosystems Eng.* 112(1), 6-13. DOI:10.1016/j.biosystemseng.2012.01.004

Mandal, A., and Chakrabarty, D. (2011). "Isolation of nanocellulose from waste sugarcane bagasse (SCB) and its characterization," *Carbohydr. Polym.* 86(3), 1291-1299. DOI:10.1016/j.carbpol.2011.06.030

Mohamed, M. A., Salleh, W. N. W., Jaafar, J., Asri, S. E. A. M., and Ismail, A. F. (2015). "Physicochemical properties of "green" nanocrystalline cellulose isolated from recycled newspaper," *RSC Adv.* 2015(5), 29842- 29849. DOI:10.1039/C4RA17020B

Moon, R. J., Martini, A., Nairn, J., Simonsen, J., and Youngblood, J. (2011). "Cellulose nanomaterials review: Structure, properties and nanocomposites," *Chem. Soc. Rev.* 40(7), 3941-3994. DOI:10.1039/C0CS00108B

Nishiyama, Y., Sugiyama, J.Chanzy, H., and Langan, P. (2003). "Crystal structure and hydrogen bonding system in cellulose Iα from synchrotron X-ray and neutron fiber diffraction," *J. Am. Chem. Soc*. 125(47), 14300-14306. DOI:10.1021/ja037055w

Nishino, T., Matsuda, I., and Hirao, K. (2004). "All-cellulose composite," *Macromolecules* 37(20), 7683-7687. DOI:10.1021/ma049300h

Neto, W. P. F., Silverio, H. A., Dantas, N. O., and Pasquini, D. (2013). " Extraction and characterization of cellulose nano crystals from agro-industrial residues – Soy hulls," *Ind. Crops Prod*. 42, 480-488. DOI:10.1016/j.indcrop.2012.06.041.

Pirani, S., and Hashaikeh, R. (2013). "Nanocrystalline cellulose extraction process and utilization of the byproduct for biofuels production," *Carbohydr. Polym.* 93(1), 357-363. DOI:10.1016/j.carbpol.2012.06.063

Rosa, S. M., Rehman, N., de Miranda, M. I. G., Nachtigall, S. M., and Bica, C. I. (2012). "Chlorine-free extraction of cellulose from rice husk and whisker isolation," *Carbohydr. Polym.* 87(2), 1131-1138. DOI:10.1016/j.carbpol.2011.08.084

Sacui, I. A., Nieuwendaal, R. C., Burnett, D. J., Stranick, S. J, Jorfi, M., Wader, C., Foster, E. J., Olsson, R. T., and Gilman, J. W. (2014). "Comparison of the properties of cellulose nanocrystals and cellulose nanofibrils isolated from bacteria, tunicate, and wood processed using acid, enzymatic, mechanical, and oxidative methods," *ACS Appl Mater Interfaces* 6(9), 6127-6138. DOI: 10.1021/am500359f

Siró, I., and Plackett, D. (2010). "Microfibrillated cellulose and new nanocomposite materials: A review," *Cellulose* 17(3), 459-494. DOI:10.1007/s10570-010-9405-y

Sun, R., Tomkinson, J., Wang, Y., and Xiao, B. (2000). "Physico-chemical and structural characterization of hemicelluloses from wheat straw by alkaline peroxide extraction," *Polymer* 41(7), 2647-2656. DOI:10.1016/S0032-3861(99)00436-X.

Sun, X. F., Xu, F., Sun, R. C., Fowler, P., and Baird, M. S. (2005). "Characterization of degraded cellulose obtained from steam exploded wheat straw," *Carbohydr. Res*. 340(1), 97-106. DOI:10.1016/j.carres.2004.10.022.

Terinte, N., Ibbett, R., and Schuster, K. C. (2011). "Overview on native cellulose and microcrystalline cellulose I structure studied by X-ray diffraction (WAXD): Comparison between measurement techniques," *Lenzinger Berichte* 89, 118-131.

Tang, A. M., Zhang, H. W., Chen, G., Xie, G. H., and Liang, W. Z. (2005). "Influence of ultrasound treatment on accessibility and regioselective oxidation reactivity of cellulose," *Ultrason. Sonochem.* 12(6), 467-472. DOI: 10.1016/j.ultsonch.2004.07.003.

Tang, L., Huang, B., Lu, Q., Wang, S., Ou, W., Lin, W., and Chen, X. (2013). "Ultrasonication-assisted manufacture of cellulose nanocrystals esterified with acetic acid," *Bioresour Technol* 127, 100-105. DOI:10.1016/j.biortech.2012.09.133

Tischer, P. C. F., Sierakowski, M. R., Westfahl Jr, H., and Tischer, C. A. (2010). "Nanostructural reorganization of bacterial cellulose by ultrasonic treatment," *Biomacromolecules* 11(5), 1217-1224. DOI:10.1021/bm901383a

Wang, L. S., Zhang, Y. Z., Gao, P. J., Shi, D. X., Liu, H. W., and Gao, H. J. (2006). "Changes in the structural properties and rate of hydrolysis of cotton fibers during extendedenzymatic hydrolysis," *Biotechnol Bioeng* 93(3), 443-456. DOI:10.1002/bit.20730

Yahya, M., Lee, H. V., and Abd Hamid, S. B. (2014). "Preparation of nanocellulose *via* transition metal salt catalyzed hydrolysis pathway," *BioResources* 10(4), 7627-7639.

Yousefi, H., Nishino, T., Faezipour, M., Ebrahimi, G., and Shakeri, A. (2011). "Direct fabrication of all-cellulose nanocomposite from cellulose microfibers using ionic liquid-based nanowelding," *Biomacromolecules* 12(11), 4080-4085. DOI:10.1021/bm201147a

Zaman, M., Xiao, H., Chibante, F., and Ni, Y. (2012). "Synthesis and characterization of cationically modified nanocrystalline cellulose," *Carbohydr. Polym.* 89(1), 163-170. DOI:10.1016/j.carbpol.2012.02.066

Article submitted: June 16, 2015; Peer review completed: November 1, 2015; Revised version received and accepted: November 30, 2015; Published: March 10, 2016.
DOI: 10.15376/biores.11.2.3840-3855